Metastability in correlated electron systems

Dynamical mean-field approach to correlated electron superconductivity and metastability in real materials

***N. Witt, L. Bremer, T. O. Wehling**, I. Institut für Theoretische Physik, Universität Hamburg*

In Short

- Study of spatial coherence in unconventional, electron correlated superconductivity
- C_{60} based materials show a rich phase diagram suited for investigation of metastability during first order phase transitions
- Motivated by metastable, photoinduced superconductivity known from experiment
- Investigating unstable solutions around phase transitions with new computational methods

Many complex phenomena and competing phases appear in materials with strong electron correlations, like Mott-insulating behavior, charge density waves, or magnetic order. In addition, unconventional superconductivity emerges in many strongly correlated materials, a state of matter with zero electrical resistance, perfect diamagnetic properties, and macroscopic quantum coherence. Over time, many materials have been found that show this complex state of matter. Examples range from heavy fermion compounds, cuprates, and organic conductors to potentially more recent findings in magic angle twisted bilayer graphene and nickelate materials.

The physics in these systems is governed by spatiotemporal fluctuations linked to the coherence of the macroscopic condensate. Central to its characterization is the knowledge of the fundamental length sccales of a superconductor, the coherence length ξ and the penetration depth λ. While ξ specifies the relevant length scales for fluctuations pertinent to, e.g., the formation of vortex lattices or magneto-thermal transport, the penetration depth determines how far magnetic fields can penetrate superconducting matter. Together, they determine the properties of superconductor like, e.g., the classification into type I and type II superconductors, which is important for tayloring superconducting devices for applications in novel nanostructures, measuring devices or quantum computing.

In our work [2], we developed a framework to directly calculate the coherence length for superconductors with strong electron correlations from microscopic theories and first principles. It is based on superconducting pairs with finite-momentum illustrated in Figure 1 where the order parameter of the

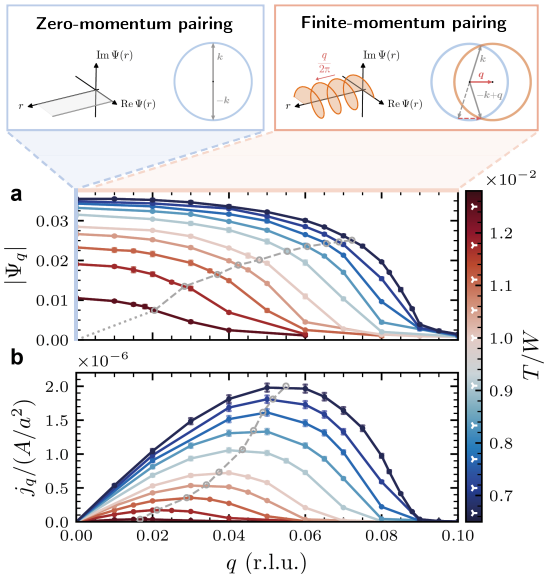

Figure 1: Influence of finite-momentum pairing (FMP) constraint on the superconducting condensate. *The top panel insets sketch the position and momentum space representation of the order parameter(OP) $\Psi_q(r) = |\Psi_q|e^{iqr}$ in the zero-momentum (left, $q = 0$) and finite-momentum pairing states (right, $q > 0$). The main panels show (a) the momentum dependence of the OP modulus and (b) the supercurrent density j_q as function of Cooper pair momentum q in reciprocal lattice units (r.l.u.). Gray lines indicate the points of extracting ξ and the depairing current j_{dp}, the maximal achievable current connecting to λ (see the paper in [2] for more information). The color bar shows different temperatures T with white triangular markers. This figure is Fig. 2 of our work [2].*

superconducting state has a spatially varying phase $e^{i\mathbf{qr}}$ with wave momentum q and position r. Due to this phase, the Cooper pairs forming the superconducting condensate gain a finite center-of-mass momentum corresponding to supercurrent flow that increases the kinetic energy and hence reduces the binding energy. The analysis of the order parameter, that gets suppressed for finite q, and the supercurrent directly give access to ξ and λ.

We embedded this novel approach in dynamical mean-field theory (DMFT), a strong coupling approach to describe many-body physics of strongly correlated and localized electrons [1], and applied it to the material family of alkali doped fullerides (A_3C_{60}) [2]. In these materials, C_{60} molecules ("Bucky balls") – carbon atoms arranged in a soccer-ball-like shape – are put in a crystaline environment. Upon doping with Alkali atoms (A=K,Cs,Rb) these materials become an isotropic s-wave superconductor with critical temperatures T_c in the range of 20-30 K [3]. Recently, the A_3C_{60} materials moved into the

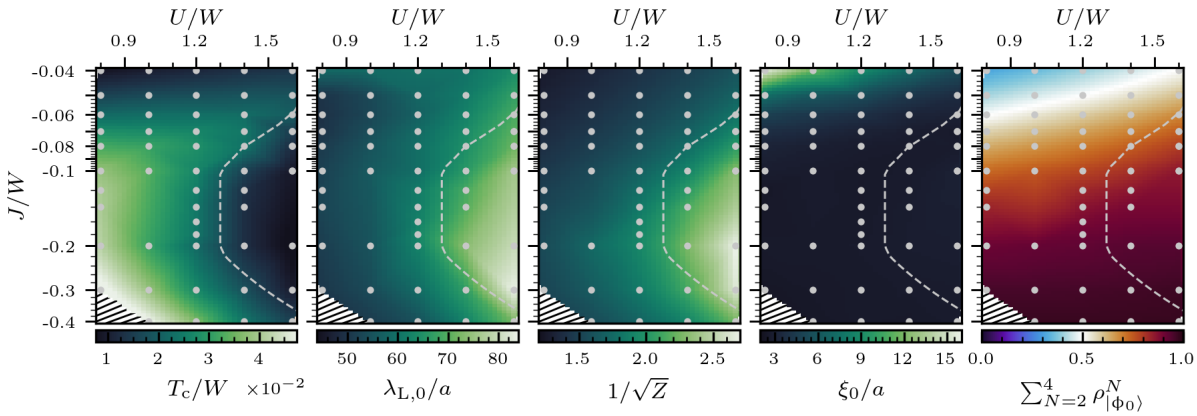

Figure 2: Superconducting state of the model in the (U, J)-interaction space. *Critical temperature , zero temperature penetration depth $\lambda_{\mathrm{L},0}$, inverse square root of quasiparticle weight Z, coherence length ξ_0, and the statistical weight $\rho^N_{|\phi_0\rangle}$ of the local lowest energy states $|\phi_0\rangle$ of the $N = 2, 3, 4$ particle sectors obeying inverted Hund's rules as a function of U and J. Gray dots show original data points used for interpolation and the dashed line indicates a region where the proximity to the Mott state leads to a suppression of the superconducting state. We find an enhancement of T_c for increased Hund's coupling $|J|$ at small to intermediate Hubbard interactions U. There is no data point at the charge degeneracy line $U = 2|J|$ in the lower left corner as marked by black 'canceling' lines. This figure is panel **a** in Fig. 4 of our work [2].*

spotlight because the phenomenon of light-induced superconductivity was discovered [4–6].

We want to highlight two key results of this work: First, our theoretical calculations of ξ and λ for *ab initio* estimated interaction parameters linking to A_3C_{60} are in very good agreement with experimental measurements, validating our approach. Second, we find a region of enhanced, localized superconductivity by increasing inverted Hund's coupling $J < 0$ that sets the pairing strength (Figure 2). This strong-coupling regime is characterized by a plateau of short coherence length and increasing critical temperatures (T_c), while maintaining a high phase stiffness $D_\mathrm{s} \propto \lambda^{-2}$, responsible for the macroscopic coherence of the condensate.

Our results are unexpected, as the increase of pairing strength typically compromises condensate stiffness and suppresses T_c. In our work [2] we discuss these results in the context of the lattice BCS-BEC crossover phenomenology, which explains this relation and, in our current understanding, sets a limit on the maximally achievable performance of superconducting matter. We explain how multiorbital physics as present in A_3C_{60} allows for a circumvention of these limitations. Thus, our results provide a promising route for achieving higher critical temperatures, critical currents and critical fields.

Our future goal is to further investigate the phase diagram of A_3C60. Specifically, we aim to study phase transitions in this system with regard to metastable states. Our interest in this area is particularly piqued by the discovery of photoinduced superconductivity in this material, as mentioned above [4–6]. Since these transient states are rapidly decaying, it is promising to delve into the topic of metastability in these materials and correlated electron systems in general. To this end, we are extending our code with an algorithm capable of revealing unstable solutions in first-order phase transitions through a phase space extension, thereby contributing to a deeper understanding of these states. We have used this method to investigate metastability of Mott transition in the Bethe lattice which allowed us to follow unstable solutions and calculate Landau free energies inside the region of the phase transition (Figure 3). The phase diagram of A_3C_{60} is highly complex and thus provides numerous opportunities for investigations in this field. We intend to study two types of metastability in particular: Firstly, transitions associated with superconductivity, and secondly, metastable states occurring at Mott transitions as observed in the phase diagram [2,7].

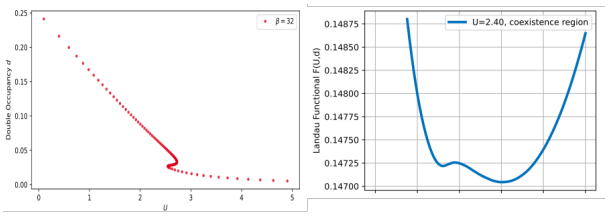

Figure 3: Metastability during Mott transition. ***Left panel****: Following an unstable solution through the coexistence region of the Mott transition for a Bethe lattice, where three solutions coexist.* ***Right panel****: Example for a Landau free energy inside the coexistence region at $U = 2.4$. The stability of each of these solutions can be investigated looking at the free Landau energies corresponding to a fixed Hubbard Interaction U. Minima indicate stable or metastable solutions while maxima indicate unstable solutions.*

WWW

https://www.physik.uni-hamburg.de/en/th1/ag-wehling.html

More Information

[1] A. Georges, G. Kotliar, W, Krauth, M. J. Rozenberg, *Rev. Mod. Phys.* **68**, 13 (1996) doi: 10.1103/revmodphys.68.13

[2] N. Witt, Y. Nomura, S. Brener, R. Arita, A. Lichtenstein, T. O. Wehling arXiv:2310.09063 (2023). doi:10.48550/arXiv.2310.09063

[3] R. H.Zadik, Y. Takabayashi, G. Klupp, R. H. Colman, A. Y. Ganin, A.Potocňik, P. Jeglič, D. Arčon, P. Matus, K. Kamarás, Y. Kasahara, Y. Iwasa, A. N. Fitch, Y. Ohishi, G. Garbarino, K. Kato, M. J. Rosseinsky, K. Prassides *Science Adv.* **1** (2015). doi: doi:10.1126/sci- adv.1500059

[4] M. Mitrano, A. Cantaluppi, D. Nicoletti, S. Kaiser, A. Perucchi, S. Lupi, P. Di Pietro, D. Pontiroli, M. Riccò, S. R. Clark, D. Jaksch, A. Cavalleri *Nat. Phys.* **530**, 461 (2016). doi: doi: 10.1038/nature16522

[5] M. Buzzi, D. Nicoletti, M. Fechner, N. Tancogne-Dejean, M. A. Sentef, A. Georges, T. Biesner, E. Uykur, M. Dressel, A. Henderson, T. Siegrist, J. A. Schlueter, K. Miyagawa, K. Kanoda, M.-S. Nam, A. Ardavan, J. Coulthard, J. Tindall, F. Schlawin, D. Jaksch, A. Cavalleri *Phys. Rev. X* **10**, 031028 (2020). doi:doi:10.1103/physrevx.10.031028

[6] M. Budden, T. Gebert, M. Buzzi et al. *Nat. Phys.* **17**, 611–618 (2021). doi: 10.1038/s41567-020-01148-1

[7] S. Hoshino, P. Werner *Phys. Rev. Lett.* **17** 177002 (2017). doi:10.1103/PhysRevLett.118.177002

Project Partners

Y. Nomura (U Tohoku), R. Arita (U Tokyo), A. L. Lichtenstein (U Hamburg), M. Eckstein (U Hamburg), H. Strand (U Örebrö)

Funding

DFG funded Cluster of Excellence “CUI: Advanced Imaging of Matter” (EXC 2056) – project ID 390715994

DFG Subject Area

3.21-02